

# SUPER-RESOLUTION MAPPING OF LANDSCAPE OBJECTS FROM COARSE SPATIAL RESOLUTION IMAGERY

A. M. Muad\* and G. M. Foody

School of Geography, University of Nottingham, Nottingham, NG7 2RD, UK  
lgxamm@nottingham.ac.uk

**KEY WORDS:** Super-resolution mapping, coarse spatial resolution image, landscape patches characterization

## ABSTRACT:

The landscape patches that are fundamental to landscape ecology may be considered as objects to be extracted from remotely sensed imagery. The accuracy with which objects may be characterised varies as a function of the spatial resolution of the imagery used. In general terms, a coarsening of the spatial resolution degrades the characterization of objects, notably through an increase in the proportion of mixed pixels which cannot be appropriately represented by conventional hard classification techniques. Accurate landscape mapping may often require either the adoption of fine spatial resolution imagery or use of sub-pixel scale analyses of coarse spatial resolution imagery. As the former is often impractical, the full realization of the potential of remote sensing as a source of information on landscape objects requires developments in sub-pixel scale techniques. In this paper, a new method of super-resolution mapping based on a unifying framework of image halftoning, inverse halftoning and Hopfield neural network techniques is proposed as a means of gaining accurate information on landscape patches from coarse spatial resolution images. Fine temporal resolution of coarse spatial resolution remote sensing systems is exploited by fusing the time-series data as an input for the super-resolution mapping. The accuracy of the analyses is evaluated relative to conventional a hard classification technique using object characterization. The results show that the proposed hybrid method is considerably more accurate than standard hard analyses in estimating the shape of the objects. The results also demonstrate that objects that are smaller than a pixel, which are missed using the hard classification techniques, can be detected using the super-resolution mapping.

## 1. INTRODUCTION

The landscape patches that are distributed spatially on the Earth's surface are very essential in studies related to ecology and geography. The nature of the landscape patches may influence ecological processes that occur or evolve in an area. One of the ways to study the landscape patches is by observing them with remote sensing imagery. Through remote sensing imagery, landscape patches can be extracted and treated as objects. Several physical characteristics such as area, perimeter, shape, orientation and spatial formation can be calculated from an object. The accuracy with which objects may be characterised varies as a function of the spatial resolution of the imagery used. Relatively, the accuracy obtained in fine spatial resolution imagery is higher than coarse spatial resolution imagery.

Although fine spatial resolution imagery provides detailed information, such imagery may be unavailable and expensive. Moreover, the image extent is not large. Alternatively, a low-cost solution to acquiring landscape information can be realized by exploiting the information content of coarse spatial resolution imagery. The size of an area covered by this imagery is large. However, the coarse spatial resolution imagery contains a higher proportion of mixed pixels than pure pixels. In this sense, a mixed pixel is a pixel that contains several classes of land cover whereas a pure pixel only occupies a single class.

Various types of land cover can be distinguished using land cover classification techniques. Conventional hard classification techniques tend to map a mixed pixel into one specific class

which represents the highest proportion of the class within the pixel while ignoring other classes. Consequently, this approach could deteriorate the quality of landscape patch appearances in the coarse spatial resolution imagery. To allow a pixel to accommodate more than one land cover class, a classification scheme that is able to map land cover classes at the sub-pixel scale is required.

Super-resolution mapping is a technique which allows mapping at the sub-pixel scale. Several super-resolution mapping techniques have been proposed such as spatial dependence maximisation (Atkinson, 1997), sub-pixel per-classification (Aplin and Atkinson, 2001), linear optimisation technique (Verhoeve and De Wulf, 2002), Hopfield neural network (Tatem et al., 2001a; Tatem et al., 2001b; Tatem et al., 2002), two-point histogram optimisation (Atkinson, 2008), genetic algorithms (Mertens et al., 2003), wavelet coefficients prediction using feed-forward neural networks (Mertens et al., 2004) and pixel swapping (Thornton et al., 2006). All of these techniques take a single coarse spatial resolution image as their input. Although they may be used to derive a map at a finer spatial scale than the input imagery, there are many concern with their use.

Additional information, normally a finer spatial resolution image can be incorporated into the super-resolution mapping to increase the accuracy of land cover mapping and to decrease the uncertainty of locating the land cover (Nguyen et al., 2006). Amongst the additional information that have been used in the super-resolution mapping are LIDAR (Nguyen et al., 2005), geo-statistical data (Boucher and Kyriakidis, 2006), fused

---

\* Corresponding author.

images (Nguyen et al., 2006) and panchromatic imagery (Atkinson, 2008). Fine spatial resolution remote sensing systems such as SPOT 5, IKONOS and QuickBird provide both multispectral and panchromatic imagery. The panchromatic images usually have finer spatial resolution than the multispectral images.

However, not all remote sensing systems are able to acquired finer spatial resolution image along with the main imagery. Coarse spatial resolution remote sensing systems such as MODIS, MERIS and AVHRR are not designed to capture panchromatic images. Exploiting the fine temporal resolution of these systems may solve the problem of acquiring additional information. The fine temporal repeat cycle of these systems enables time-series images of a same spatial resolution to be combined together. The fine temporal resolution characteristic of these systems may confine from acquiring significant changes on the Earth's surface that might be occurred if the observation of the satellite systems takes a long period of time.

The imagery of a site acquired on different dates typically differs in subtle ways, with the location of pixels varying slightly due to, for example, minor orbital translations of remote sensing satellites. The slight differences between images can be exploited by combining a time-series coarse spatial resolution images into an integrated image which may contain more information than a single coarse spatial resolution image (Packalen et al., 2006).

The aim of this paper is to estimate accurate landscape patches characterization by combining multiple coarse spatial resolution images. A new super-resolution mapping algorithm will be presented which is suitable for processing multiple input images of the same spatial resolution. Results will be presented based on patch or object characterization.

## 2. STUDY AREA AND DATASETS

The study area covers approximately a 20km<sup>2</sup> area located in Quebec province, Canada. It is situated between latitudes 55°08'35"N and 55°06'08"N and between longitudes 77°41'39"W and 77°36'30"W. The area that is near the Hudson Bay contains an abundance of lakes of various size, shape, orientation and spatial formations. Landsat ETM+ near IR band image with a spatial resolution of 30m of this area was used since land and water are very separable in this band. Figure 1 shows the image of the area.

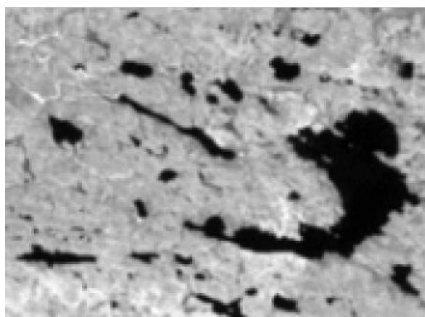


Figure 1. Landsat ETM+ near IR band image of 30m per pixel

In this study, we modelled multiple time-series observations of remote sensing imagery by generating multiple coarse spatial resolution images from a fine spatial resolution image in Figure 1. The image in Figure 1 was down-sampled by a factor of 8 to a spatial resolution of 240m pixel. To model the slight orbital

translations, the initial position of an image for the down-sampling operation was sub-pixel shifted randomly in horizontal and vertical directions from one image to another (Lu and Inamura, 2003). Figure 2 shows one of the simulated coarse spatial resolution images.

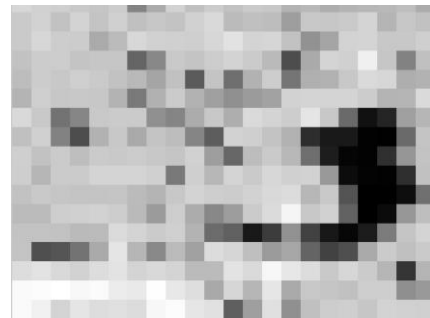


Figure 2. One of the simulated coarse spatial resolution images with a spatial resolution of 240m

## 3. METHODOLOGY

In this study, a new super-resolution mapping algorithm is proposed based on a unifying framework consisting of an image halftoning method (Lau and Arce, 2001), inverse halftoning (Venkata et al., 1998) and an active surface threshold optimized by a Hopfield neural network (Shen and Ip, 1997). Figure 3 illustrates a graphical flowchart of the new super-resolution mapping algorithm. The algorithm begins in Step 1 with an acquisition of a time-series coarse spatial resolution images. In Step 2, all the images were soft classified using a fuzzy membership function (Foody et al., 2005) to produce proportion images. In Step 3, every pixel in a proportion image was subdivided into a matrix of sub-pixels by creating repetitive information obtained from the original pixel (Fisher, 1997).

All the proportion image that differ slightly from one to another in the time series data were assumed to be translated linearly (e.g. horizontal and vertical) in a sub-pixel scale. The amount of sub-pixel shifting was calculated using an iterative back-projection method (Irani and Peleg, 1991) and was used to counterbalance the position of every image before being combined into a fused image as shown in Step 4. This step was implemented to ensure that information from multiple images can be set in the correct location.

Land cover classification divides different types of land cover in an image. Because only two types of land cover class (land and water) that need to be classified, a binary conversion of the fused image is required. Several super-resolution mapping techniques (Tatem et al., 2001a; Tatem et al., 2001b; Tatem et al., 2002; Thornton et al., 2006) assign binary representatives based on a proportion of land cover within a pixel of a coarse spatial resolution image. In the earliest stage of those techniques, the binary representatives are assigned as values for sub-pixels of a coarse spatial resolution image. The arrangement of the binary values for the sub-pixels that appear to be a dot pattern is completely random. Unlike the existing techniques, our method arranged the binary representatives for sub-pixels using an error diffusion technique (Floyd and Steinberg, 1976), which is a popular dithering technique in image halftoning operations as shown in Step 5. Then, using an inverse halftoning, the dot pattern created by error diffusion techniques in the binary image can be converted back into a continuous gray level image a shown in Step 6. The gray level image was fed into a Hopfield neural network to generate an optimized

threshold using a paradigm of an active surface image as shown in Step 7. Finally, in the Step 8, the continuous image in Step 6 was compared with the active surface image in Step 7 to classify the land cover into two different classes: land and water.

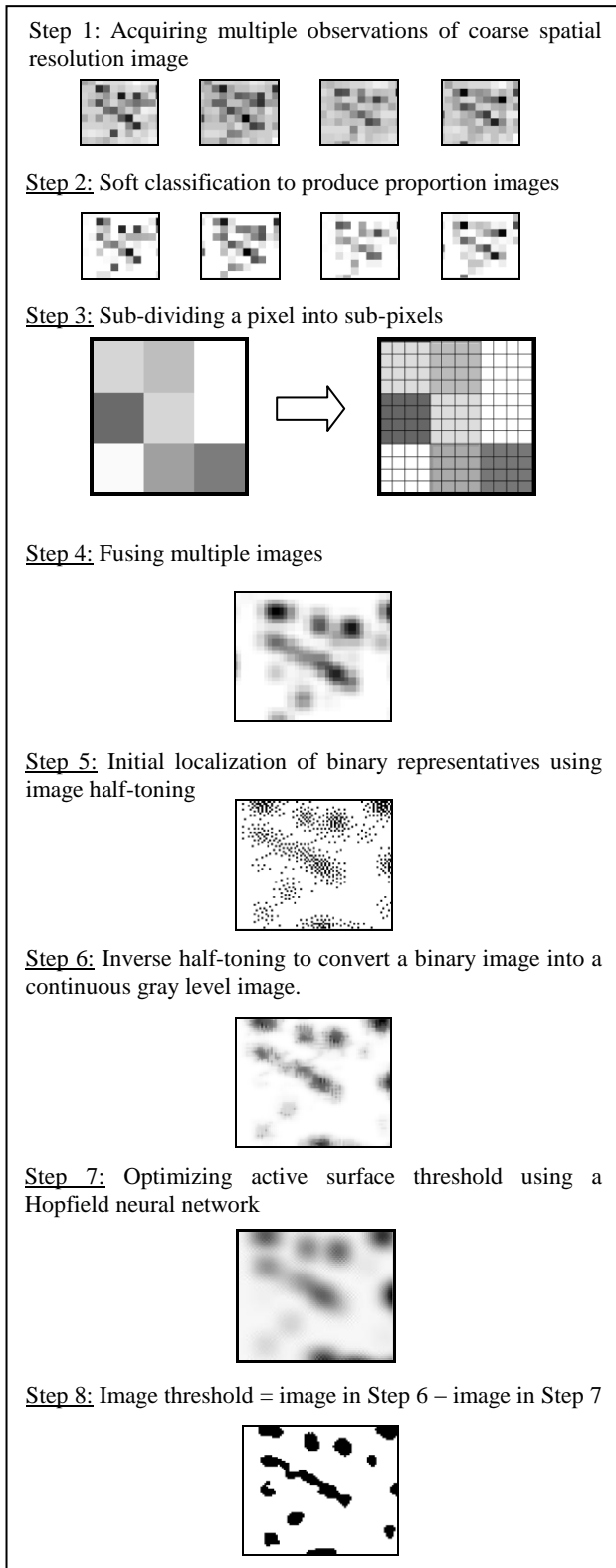


Figure 3. Flowchart of the proposed super-resolution mapping algorithm procedure

#### 4. SHAPE CHARACTERIZATION

Object shape may be characterized in many ways (Nixon and Aguado, 2002). Here the shape of objects was characterized by area, perimeter, circularity, length and orientation. Figure 4 illustrates an example of shape characterization for an object. The area of an object was determined by measuring the quantity of pixels assigned for the object, while the number of pixels at the boundary of the object determines its perimeter.

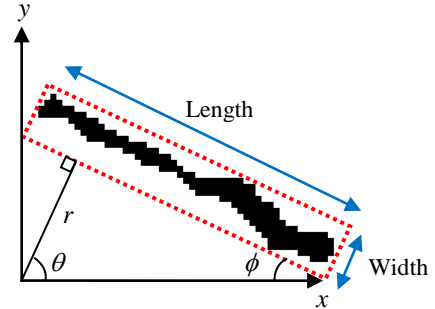


Figure 4. Object characterization

The circularity of an object is calculated by circularity index as

$$\omega = \frac{4\pi A}{P^2} \quad (1)$$

where A is area and P is perimeter. The index ranges from 0 to 1, where values approaching 1 indicate that the shape is circular while values approaching 0 are used to represent that the shape is linear. The orientation of an object is calculated using Hough transform (Duda and Hart, 1972; Hough, 1962).

$$r = x \cos \theta + y \sin \theta \quad (2)$$

$$\phi = \theta - 90^\circ \quad (3)$$

The sign of the orientation indicates the direction of the object.

#### 5. RESULTS AND DISCUSSION

Results of the super-resolution mapping method were evaluated in terms of visual appearance, overall and individual lake characterizations. Figure 5 shows result of land cover classification applied on the (a) fine spatial resolution image of Figure 1, (b) a coarse spatial resolution using conventional hard classification, and (c) a combination of multiple coarse images using the proposed super-resolution mapping method. For comparative purpose, image in Figure 5(a) was referred as a reference image. In Figure 5 two types of land cover were distinguished; land (white) and water (black).

Visual comparison between the hard classified image (Figure 5(b)) and super-resolution mapped image (Figure 5(c)) displays noticeable different in terms of the shape of the lakes and the number of the lakes. In the hard classified image, the shape of lakes appears to be blocky and suffered from a pixellation effect. In contrast, the shape of lakes in the super-resolution mapped image exhibits smooth boundaries. The resemblance between shapes in the super-resolution mapped image and the reference image is visibly closer than the shape of lakes in the hard classified image.

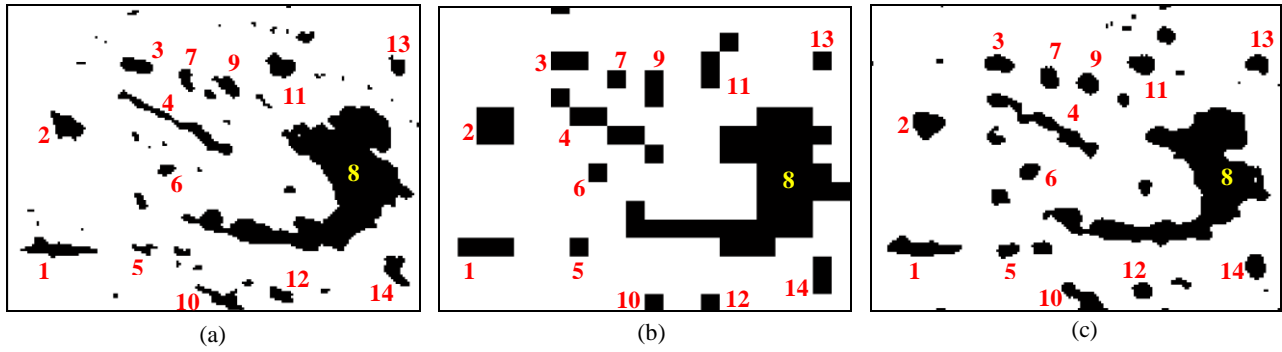


Figure 5. Land cover classification (a) on a reference image; (b) on a coarse spatial resolution image using hard classification method; and (c) multiple coarse spatial resolution images using the proposed super-resolution mapping method

Lake	Area		Perimeter		Circularity		Length		Orientation	
	HC	SRM	HC	SRM	HC	SRM	HC	SRM	HC	SRM
1	51.12	30.00	13.14	3.10	0.29	0.09	11.00	0.95	0.00	3.00
2	144.00	9.75	17.44	6.76	0.14	0.32	1.00	1.00	33.00	20.00
3	54.00	2.25	13.27	1.76	0.07	0.11	2.00	1.00	6.00	0.00
4	192.75	71.88	30.70	8.82	0.04	0.03	1.61	2.07	1.00	2.00
5	34.13	17.13	1.86	1.66	0.37	0.31	3.03	1.03	4.00	0.00
6	35.25	23.13	8.69	1.83	0.12	0.37	0.00	1.00	16.00	10.00
7	19.75	21.88	1.27	4.59	0.20	0.08	2.00	0.00	66.00	22.00
8	388.90	332.70	53.91	38.25	0.07	0.00	4.04	2.25	16.00	1.00
9	64.25	5.75	9.44	3.76	0.16	0.18	4.00	2.00	127.00	7.00
10	26.75	24.38	33.63	8.83	0.52	0.18	15.38	0.69	25.00	2.00
11	101.50	12.25	40.54	2.27	0.36	0.17	13.84	3.00	82.00	4.00
12	14.13	1.00	1.66	6.93	0.23	0.34	2.00	1.00	31.00	14.00
13	22.25	23.38	6.93	5.73	0.05	0.03	1.00	1.00	58.00	37.00
14	39.75	11.13	1.544	12.485	0.18	0.33	3.00	2.00	142.00	28.00
$\Sigma$	1188.52	586.58	234.03	106.75	2.81	2.54	63.90	18.99	607.00	150.00

Table 1. Comparison of lake characterization in the hard classified (HC) image and the super-resolution mapped (SRM) image

In terms of the number of lakes, the super-resolution mapping approach provided a representation for 36 of the 48 shown in the reference image. Only 15 lakes were found in the hard classified image. The size of the lakes that are missed in the hard classified image is smaller than a size of a pixel of a coarse spatial resolution image. In the super-resolution mapped image, several lakes that are smaller than a pixel of a coarse spatial resolution image are detectable although the quantity is not as many as in the reference image. Overall, the percentage of area for a land cover that is classified as water in the reference image is 14.72%, hard classified image (19.00%), and super-resolution mapped image (14.57%).

There were 15 lakes detected in the hard classified image. One of them is located at the top edge of the image. This lake was ignored in the lake characterization analysis because its shape is incomplete. The remaining 14 lakes and their corresponding lakes in the reference image and in the super-resolution mapped image were indexed numerically for a comparative study of the lake characterization.

Shape characterization analysis on the indexed lakes in each Figure 5 was summarized in Table 1. Each lake was characterized by area, perimeter, circularity, length and orientation. The column for each character in the Table 1 is further divided into two to describe the difference of shape characterization measured from the hard classified and the super-resolution mapped images. Each shape characteristic in both images was compared against the corresponding characteristic in the reference image. The magnitude of residual values for the comparison is given in Table 5. In general, shape characterization of lakes in the super-resolution mapped image tends to produce less error than the characterization in the hard classified image.

Four types of shape characteristics: area, perimeter, length and orientation display considerable wide margins between results in the hard classified image and the super-resolution mapped image. In terms of circularity aspect, the margin between result of residuals in the hard classified image and the super-resolution mapped image is rather narrow. This scenario occurred because 6 from the 14 lakes in the hard classified

image produce less circularity measurement error than lakes in the super-resolution mapped image.

Apart from numerical comparisons, visual inspection on individual lake can be used to display the advantages of the super-resolution mapping method. The shape of the lakes in the super resolution mapped image tends to be preserved and displays close resemblance with the shape in the reference image. For example, in the super-resolution mapped image, the left side of lake #1 contains more area of water than in its right side. The asymmetrical feature of the lake #1 in the super-resolution mapped image is almost similar to the shape of the lake #1 in the reference image. In contrast, hard classification method interprets the lake #1 as a symmetrical lake. Another example can be seen in lake #8, where the curve of the lake's boundary in the super-resolution mapped image is curlier than the boundary of the corresponding lake in the hard classified image.

Super-resolution mapping method deals considerably better than the conventional hard classification on mixed pixel problem. Lake that is degraded by high proportion of mixed pixel such as lake #4, which lies diagonally in Figure 5, contains fewer errors in terms of area, perimeter and circularity in the super-resolution mapped image than in the hard classified image. Visually, the boundary of the lake #4 in the super-resolution mapped image is smoother than lake #4 in the hard classified image.

Using hard classification mapping, adjacent lakes that are situated close to one another tend to be merged into a large single unit lake. In the hard classified image, Lake #11 is interpreted as one unit of lake, although in the reference and super-resolution mapped images, this lake is actually constitute of two lakes. Therefore, the super-resolution mapping method is potentially more able to avoid merging of adjacent lakes than the hard classification method.

Reliance on a single input image into land cover classification operations may not be able to provide sufficient information about the contents and its location in an output image. In the hard classified image, lake #12 is located slightly lower than its corresponding lakes in the reference and the super-resolution mapped image. The offset position of the lake #12 in the hard classified image is because the hard classification method takes single coarse spatial resolution image as its input. In contrast, the proposed super-resolution mapping method fused a time-series coarse spatial resolution images, thus, avoiding a problem of the slight shifted position and increasing the certainty of land cover location.

Further analysis was done on lakes that were omitted from the hard classified image but were detected in the super-resolution mapped image. To highlight those lakes, other irrelevant lakes were represented in light gray as shown in Figure 6. In general, the size of the highlighted lakes is smaller than a size of a pixel in a coarse spatial resolution image. The lakes were indexed alphabetically from lake #a until lake #g as shown in Figure 6(b) and its corresponding lakes in the reference image are shown in Figure 6(a). It should be noted that the spatial resolution of the reference and the super-resolution mapped images is 30m per pixel, whereas the spatial resolution of a coarse spatial resolution image is 240m per pixel. The smallest lake that can be detected by super-resolution mapping method is lake #a. The characteristics of this lake in the reference image are: 3600m<sup>2</sup> (area); 300m (perimeter); 0.50 (circularity); 180m

(length); and 0° (orientation). The characteristics of lake #a in the super-resolution mapped image are: 5400m<sup>2</sup> square pixels (area); 300m (perimeter); 0.75 (circularity); 150m (length); and 0° (orientation). Based on the comparison on these values and on visual appearance, the super-resolution mapping method was able to estimate a land cover mapping for lakes that are smaller than a size of a coarse spatial resolution image pixel markedly.

The proposed super-resolution mapping method may be able to estimate the area and perimeter of a lake and produce results that are almost identical with the reference image smaller than a size of a pixel of a coarse spatial resolution image. However, one of the limitations of this method is that it may not be able to estimate the exact shape of lakes. The shape of the lake #g in the super-resolution mapped image is less than it should be as in the reference image. The effect of this limitation is that it tends to expand the size of lakes such as lakes #b, #c, #d, #e, #f, and #h. Although the proposed method may not be able to reconstruct the exact shape of lake, the technique demonstrated reasonable results of estimating the shape of the lakes at the sub-pixel scale of a coarse spatial resolution image.

Ellipse X in Figure 6(a) contains three small lakes in the reference image, while ellipse X in Figure 6(b) contains an estimation of those lakes in the super-resolution mapped image. The location of a lake that is situated in the middle of the ellipse is approximately comparable in the two images. The result of the super-resolution mapping caused other lake in the super-resolution mapped image to be fragmented into two, although their location is approximately the same compare to the location of their corresponding lake in the reference image. The shape of the third lake in the circle X of the reference image is well estimated in the super-resolution mapped image, but not located in the exact position.

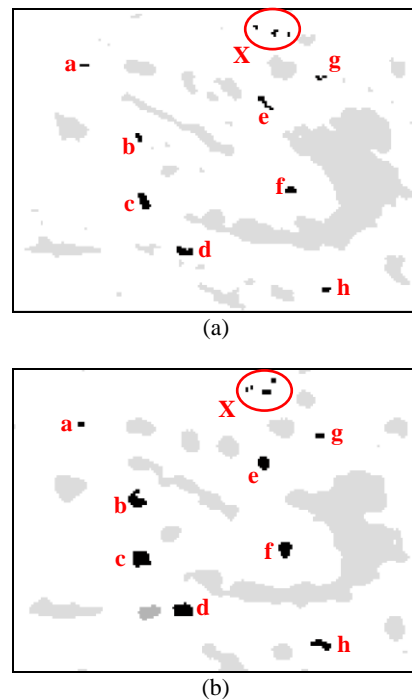


Figure 6. Object characterizations on small lakes that are omitted in the hard classified image. (a) A reference image, (b) a super-resolution mapped image

## 6. CONCLUSION

This paper proposes a new super-resolution mapping algorithm exploiting the multiple coarse spatial resolution images of a site in a time-series manner. The proposed method unified an image halftoning method, inverse halftoning and an active surface threshold which is optimized by a Hopfield neural network. The super-resolution mapping method was validated with a paradigm of object orientation using shape characteristics of a number of lakes. In all the evaluation series, the proposed super-resolution mapping method demonstrated greater capability than the conventional hard classification method by producing higher accuracy of characterizing landscape patches at the sub-pixel scale. The ability of the super-resolution mapping method to map land cover at the sub-pixel scale enhances the value of coarse spatial resolution images. The potential of this method will be beneficial to ecological and morphological studies.

## ACKNOWLEDGEMENT

The authors wish to express their gratitude to Ministry of Higher Education Malaysia and Universiti Kebangsaan Malaysia for sponsoring A.M. Muad's PhD study at University of Nottingham, UK.

## REFERENCES

- Aplin, P. and Atkinson, P.M., 2001. Sub-pixel land cover mapping for per-field classification. *International Journal of Remote Sensing*, 22(14), pp. 2853-2858.
- Atkinson, P.M., 1997. Mapping sub-pixel boundaries from remotely sensed images, In: Kemp, Z., Editor, *Innovations in GIS IV*. Taylor and Francis, London, pp. 166-180.
- Atkinson, P.M., 2008. Super-resolution mapping using the two-point histogram and multi-source imagery. In: A. Soares, M.J. Pereira and R. Dimitrakopoulos (Editors), *geoENV VI - Geostatistics for Environmental Applications* Springer Netherlands, pp. 307-321.
- Boucher, A. and Kyriakidis, P.C., 2006. Super-resolution land cover mapping with indicator geostatistics. *Remote Sensing of Environment*, 104, pp. 264-282.
- Duda, R.O. and Hart, P.E., 1972. Use of the Hough transformation to detect lines and curves in pictures. *Communicaton of the ACM*, 15(1), pp. 11-15.
- Fisher, P., 1997. The pixel: a snare or a delusion. *International Journal of Remote Sensing*, 18, pp. 679-685.
- Floyd, R.W. and Steinberg, L., 1976. An adaptive algorithm for spatial grey scale, *Proceedings of the Society of Information Display*, pp. 75-77.
- Foody, G.M., Muslim, A.M. and Atkinson, P.M., 2005. Super-resolution mapping of the waterline from remotely sensed data. *International Journal of Remote Sensing*, 26(24), pp. 5381-5392.
- Hough, P.V.C., 1962. *Method and means for recognizing complex patterns*. U.S. Patent 3069654, December 18, 1962.
- Irani, M. and Peleg, S., 1991. Improving resolution by image registration. *Computer Vision, Graphics and Image Processing: Graphical Models and Image Processing*, 53(3), pp. 231-239.
- Lau, D.L. and Arce, G.R., 2001. *Modern Digital Halftoning*. Marcel Dekker, Inc., New York.
- Lu, Y. and Inamura, M., 2003. Spatial resolution improvement of remote sensing images by fusion of subpixel-shifted multi-observation images. *International Journal of Remote Sensing*, 24(23), pp. 4647-4660.
- Mertens, K.C., Verbeke, L.P.C., Ducheyne, E.I. and Wulf, R.R.D., 2003. Using genetic algorithms in sub-pixel mapping. *International Journal of Remote Sensing*, 24(21), pp. 4241-4247.
- Mertens, K.C., Verbeke, L.P.C., Westra, T. and Wulf, R.R.D., 2004. Sub-pixel mapping and sub-pixel sharpening using neural network predicted wavelet coefficients. *Remote Sensing of Environment*, 91, pp. 225-236.
- Nguyen, M.Q., Atkinson, P.M. and Lewis, H.G., 2005. Superresolution mapping using a Hopfield neural network with LIDAR data. *IEEE Geoscience and Remote Sensing Letters*, 2, pp. 366-307.
- Nguyen, M.Q., Atkinson, P.M. and Lewis, H.G., 2006. Superresolution mapping using a Hopfield neural network with fused images. *IEEE Transactions on Geoscience and Remote Sensing*, 44(3), pp. 736-749.
- Nixon, M.S. and Aguado, A.S., 2002. *Feature Extraction and Image Processing*. Newnes, Oxford
- Packalen, P., Tokola, T., Saastamoinen, J. and Maltamo, M., 2006. Use of a super-resolution method in interpretation of forests from multiple NOAA/AVHRR images. *International Journal of Remote Sensing*, 27, pp. 5341-5357.
- Shen, D. and Ip, H.H.S., 1997. A Hopfield neural network for adaptive image segmentation: An active surface paradigm. *Pattern Recognition Letters*, 18, pp. 37-48.
- Tatem, A.J., Lewis, H.G., Atkinson, P.M. and Nixon, M.S., 2001a. Multiple-class land-cover mapping at the sub-pixel scale using a Hopfield neural network. *International Journal of Applied Earth Observation and Geoinformation*, 3(2), pp. 184-190.
- Tatem, A.J., Lewis, H.G., Atkinson, P.M. and Nixon, M.S., 2001b. Super-resolution target identification from remotely sensed image using a Hopfield neural network. *IEEE Transactions on Geoscience and Remote Sensing*, 39(4), pp. 781-796.
- Tatem, A.J., Lewis, H.G., Atkinson, P.M. and Nixon, M.S., 2002. Super-resolution land cover pattern prediction using a Hopfield neural network. *Remote Sensing of Environment*, 79, pp. 1-14.
- Thornton, M.W., Atkinson, P.M. and Holland, D.A., 2006. Sub-pixel mapping of rural land cover objects from fine spatial resolution satellite sensor imagery using super-resolution pixel-swapping. *International Journal of Remote Sensing*, 27(3), pp. 473-491.
- Venkata, N.D., Kite, T.D., Venkataraman, M. and Evans, B.L., 1998. Fast Blind Inverse Halftoning, *IEEE International Conference on Image Processing*, Chicago, IL, USA, pp. 64-68.
- Verhoeve, J. and De Wulf, R., 2002. Land cover mapping at sub-pixel scales using linear optimization techniques. *Remote Sensing of Environment*, 79(1), pp. 96-104.